

Patch based Colour Transfer using SIFT Flow

Hana Alghamdi & Rozenn Dahyot

*School of Computer Science & Statistics
Trinity College Dublin, Ireland*

Abstract

We propose a new colour transfer method with Optimal Transport (OT) to transfer the colour of a source image to match the colour of a target image of the same scene that may exhibit large motion changes between images. By definition OT does not take into account any available information about correspondences when computing the optimal solution. To tackle this problem we propose to encode overlapping neighborhoods of pixels using both their colour and spatial correspondences estimated using motion estimation. We solve the high dimensional problem in 1D space using an iterative projection approach. We further introduce smoothing as part of the iterative algorithms for solving optimal transport namely Iterative Distribution Transport (IDT) and its variant the Sliced Wasserstein Distance (SWD). Experiments show quantitative and qualitative improvements over previous state of the art colour transfer methods.

Keywords: Optimal Transport, Nadaraya-Watson estimator, Iterative Distribution Transfer, Sliced Wasserstein Distance, Colour Transfer

1 Introduction

Colour variations between photographs often happen due to illumination changes, using different cameras, different in-camera settings or due to tonal adjustments of the users. Colour transfer methods have been developed to transform a source colour image into a specified target colour image to match colour statistics or eliminate colour variations between different photographs. Colour transfer has many applications in image processing problems, ranging from generating colour consistent image mosaicing and stitching [1] to colour enhancement and style manipulation [2].

When computing the transfer function, considering colour information only does not take into account the fact that coherent colours should be transferred to neighboring pixels, which can create results with blocky artifacts emphasizing JPEG compression blocks, or increase noise. To tackle this problem, Alghamdi et al. [3] proposed the Patch based Colour Transfer (PCT_OT) approach that encodes overlapping neighborhoods of pixels, taking into account both their colour and pixel positions. PCT_OT algorithm shows improvement over the state of the art methods but also shows limitations by creating shadow artifacts when there are large changes between target and source images. In this paper we propose to improve PCT_OT by first improving the data preparation step for defining patches thanks to SIFT flow [4]. We estimate motions between images using SIFT flow approach and incorporate the spatial correspondence information in the encoded overlapping neighborhoods of pixels. This formulation makes OT *implicitly* take into account correspondences information when computing the optimal solution. Our second contribution is to introduce smoothing as part of the iterative algorithms for solving optimal transport namely Iterative Distribution Transport (IDT) and its variant the Sliced Wasserstein Distance (SWD).

2 PCT_OT with SIFT Flow

2.1 Combine colour and spatial information

The spatial information for the target image is calculated using SIFT flow method which estimates dense spatial correspondences by robustly aligning complex scene pairs containing significant spatial differences [4], while

in *PCT_OT* [3] the original pixel positions in the grid coordinate of the image are used. Using correspondences will allow colour transfer between images that contain moving objects and overcome the limitations in *PCT_OT*. More specifically, let y^p be the 2D pixel position of the target image to be computed, and let $\mathbf{p} = (a, b)$ be the 2D grid coordinate of the target image and $\mathbf{w}(\mathbf{p}) = (u(\mathbf{p}), v(\mathbf{p}))$ be the flow vector at \mathbf{p} computed using SIFT flow method, then $y^p = \mathbf{p} + \mathbf{w}(\mathbf{p}) = (a + u(\mathbf{p}), b + v(\mathbf{p}))$ is the new pixel position in the target image that match a pixel position in the source image. The pixel's colour y^c and its pixel position y^p are concatenated into a vector $y = (y^c, y^p)^T$ such that $\dim(y) = \dim(y^c) + \dim(y^p)$. The source image keeps the grid coordinate of the image as pixel positions, i.e $x^p = \mathbf{p}$ and similarly to the target image the pixel's colour x^c and its pixel position x^p are concatenated into a vector $x = (x^c, x^p)^T$ such that $\dim(x) = \dim(x^c) + \dim(x^p)$.

2.2 Data normalisation

Since the colours have integer values from 0 to 255, and the spatial values can be anything depending on the size of the image. In order to produce consistent results regardless of the size of the image and better control parameters, we normalize all the colour and position coordinates to lie between 0 and 255 to create a hypercube in \mathbb{R}^d . We then stretch that space in the direction of the spatial coordinates by a factor w to make it harder to move the pixels in the spatial domain than in the colour domain, because since we are focusing on transferring colour between images of a same scene, we know that the scenes are overlapped and hence the more overlapped areas we have the higher w value we can set.

2.3 Create patch vectors

Similarly to *PCT_OT* [3] we encode overlapping neighborhoods of pixels to preserve local topology information. Starting from the origin of the coordinate system of the images (upper left corner), we use a sliding window operation of window size $k \times k$ to extract overlapping patches. From each individual patch we create a high dimensional vector in $\mathbb{R}^{d \times k \times k}$. We apply this process to the source and target images to create patch vector sets $\{x_i\}$ and $\{y_j\}$ for each respectively.

3 Smoothed solution for 1D Optimal Transport

The OT problem consists of estimating the minimum cost (referred to as the Wasserstein Distance [5] or as the Earth Mover's Distance [6]) of transferring a source distribution to a target distribution. As a byproduct of OT distance estimation, the mapping ϕ itself between the two distributions is also provided. Monge's formulation of OT [5] defines the deterministic coupling $y = \phi(x)$ between random vectors $x \sim f(x)$ and $y \sim g(y)$ that capture the colour information of the source and target images respectively, and its solution minimizes the total transportation cost:

$$\operatorname{argmin}_{\phi} \int \|x - \phi(x)\|^2 f(x) dx \quad \text{such that:} \quad f(x) = g(\phi(x)) |\det \nabla \phi(x)| \quad (1)$$

with f the probability density function (pdf) of x and g the pdf of y . The solution for ϕ can be found using existing algorithms such as linear programming, and the Hungarian and Auction algorithms [7]. However, in practice it is difficult to find a solution for colour images when $\dim(x) = \dim(y) = d > 1$ as the computational complexity of these solvers increases in multidimensional spaces [8]. But for $d = 1$, with $x, y \in \mathbb{R}$, a solution for ϕ is straightforward and can be defined using the increasing rearrangement [5]:

$$\phi^{OT} = G^{-1} \circ F \quad (2)$$

where F and G are the cumulative distributions of the colour values in the source and target images respectively.

3.1 Iterative Distribution Transfer (IDT)

The 1D solution ϕ^{OT} Eq. (2) has been used to tackle problems in multidimensional colour spaces and of particular interest is the Iterative Distribution Transfer (IDT) algorithm for colour transfer proposed by Pitié et al. [9]. They proposed to iteratively project colour values $\{x_i\}_{i=1}^n$ and $\{y_j\}_{j=1}^m$ originally in \mathbb{R}^d to a 1D subspace

and solve the OT using ϕ^{OT} Eq. (2) in this 1D subspace and then propagate the solution back to \mathbb{R}^d space. This operation is repeated with different directions in 1D space until convergence. This strategy was inspired by the idea of the Radon Transform [9] which states the following proposition: if the target and source colour points are aligned in all possible 1D projective spaces, then matching is also achieved in \mathbb{R}^d space. Note that the implementation of IDT approximates F and G using cumulative histograms which can be considered as a form of quantile matching but with irregular quantile increments derived from the cumulative histograms of the source and target images - as source and target quantiles do not match exactly, interpolation can be used to compute solution [9].

3.2 Sliced-Wasserstein Distance (SWD)

The Sliced Wasserstein Distance (SWD) algorithm follows from the iterative projection approach of IDT but computes the 1D solution ϕ^{OT} with quantile matching instead of cumulative histogram matching [10, 11]. More specifically, SWD sorts the n 1D projections of the source and target images respectively to define quantiles with regular increments of size $\frac{1}{n}$ between 0 and 1 for both source and target distributions. The SWD algorithm can be computed in $\mathcal{O}(n \log(n))$ operations using a fast sorting algorithm [10]. When a small number of observations are available, using SWD is best but with a large number of observations, histogram matching with IDT is more efficient.

3.3 Smoothing ϕ^{OT} with Nadaraya Watson Estimator

Giving the correspondences $\{(x_i, y_i)\}_{i=1, \dots, n}$, the Nadaraya Watson (NW) estimator is defined as follows:

$$\mathbb{E}[y|x] = \int y p(y|x) dy = \int y \frac{p(y, x)}{p(x)} dy \simeq \frac{n^{-1} \sum_{i=1}^n y_i K_h(x - x_i)}{n^{-1} \sum_{i=1}^n K_h(x - x_i)} = \phi_h^{NW}(x) \quad (3)$$

With this form NW can be seen as locally weighted average of $\{y_i\}_{i=1, \dots, n}$, using a kernel as a weighting function where the bandwidth h is the hyperparameter or scale parameter of the kernel, the larger the value of h the more ϕ_h^{NW} gets smoother. We propose to smooth ϕ^{OT} computed in IDT or SWD by using non-parametric Nadaraya Watson estimator. At each iteration t , following the step of calculating the optimal map ϕ^{OT} , we feed the OT estimated correspondences $\{(x_i, \phi^{OT}(x_i))\}_{i=1}^n$ to NW estimator to compute a smoother OT solution, denoted as ϕ_h^{OT} , defined as follows:

$$\phi_h^{OT}(x) = \frac{\sum_{i=1}^n \phi^{OT}(x_i) K_h(x - x_i)}{\sum_{i=1}^n K_h(x - x_i)} \quad (4)$$

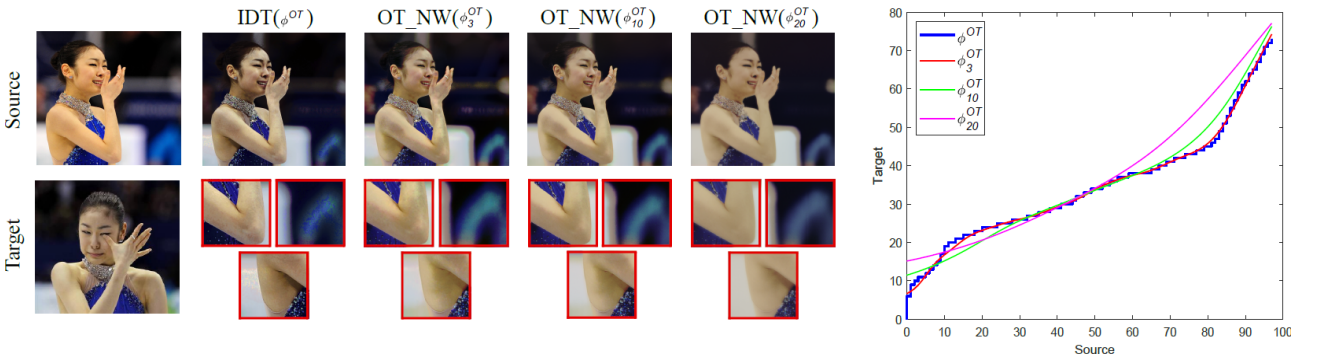


Figure 1: Results shows the smoothed Optimal Transport solution using non-parametric Nadaraya-Watson (ϕ_h^{OT}) with different bandwidth values $h = \{3, 10, 20\}$. Nadaraya-Watson significantly reduces the grainy artifacts produced by the original Optimal Transport mapping (ϕ^{OT}), the bigger h value the more smoothed mapping. The results processed without post processing step (best viewed in colour and zoomed in).

Figure 1 illustrates the effect of computing smoother OT solutions using NW with different bandwidth values on colour transfer compared with the original OT solution computed using IDT algorithm [9]. Optimal

Transport solution is suitable in situations where the function that we need to estimate must satisfy important side conditions, such as being strictly increasing, and the non-parametric NW estimator on top of the OT solution can provide the smoothness required in the estimated function. In addition, one of the important characteristics of using OT and NW estimators is that they do not assume explicit expression controlled by parameters on the regression function which makes them directly employable. In the following sections we are applying OT and NW smoothing in the relevant context of colour transfer where the the function that we need to estimate must satisfy the condition of being increasing function.

4 Experimental Assessment

We provide here quantitative and qualitative evaluations of our approach noted `OT_NW` with comparisons to different state of the art colour transfer methods noted `IDT` [9], `PMLS` [2], `GPS/LCP` and `FGPS/LCP` [12], `L2` [13] and `PCT_OT` [3]. In these evaluations we use image pairs with similar content from an existing dataset provided by Hwang et al [2]. The dataset includes registered pairs of images (source and target) taken with different cameras and settings, and different illuminations and recolouring styles.

4.1 Colour space and parameters settings

We use the RGB colour space where each pixel is represented by its 3D RGB colour values and its 2D spatial position. Our patches with combined colour and spatial features create a vector in 125 dimensions ($5 \times 5 \times 5$) for the RGB colours (3D) and position component (2D). We found patch size of 5×5 captures enough of a pixel's neighbourhood. We stretch the hypercube space in \mathbb{R}^d in the direction of the spatial coordinates by a factor $w = 10$ to make it harder to move the pixels in the spatial domain than in the colour domain. We experimented with different bandwidth values and we found a fix value of $h = 10$ gives best results.

4.2 Evaluation metrics

To quantitatively assess the recolouring results, four metrics are used: peak signal to noise ratio (PSNR) [14], structural similarity index (SSIM) [15], colour image difference (CID) [16] and feature similarity index (FSIMc) [17]. These metrics are often used when considering source and target images of the same content [18, 19, 2, 12]. Note that the results using `PMLS` were provided by the authors [2]. It has already been shown in [13] that `PMLS` performs better than two other more recent techniques using correspondences [20, 21], so `PMLS` is the one reported here with [3, 13] as algorithms that account for correspondences.

4.3 Experimental Results

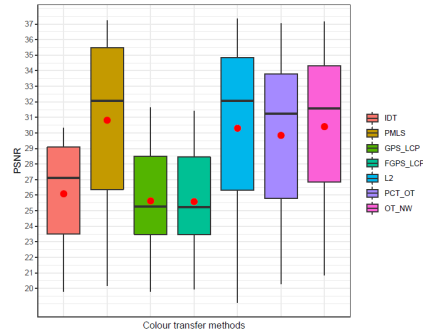
Figures 2–5 show detailed tables of quantitative results for each metric alongside with box plots carrying a lot of statistical details. The purpose of the box plots is to visualize differences among methods and to show how close our method is to the state of the art algorithms. Figure 2 (b) and Figure 5 (b) shows PSNR and FSIMc metrics results respectively, by examining the box plots in both figures we see that the four methods `PMLS`, `L2`, `PCT_OT` and `OT_NW` are greatly overlap with each other, the median and mean values (the mean shown as red dots in the plots) are the highest among all algorithms and are very close in value and the whiskers length almost similar indicating similar data variation and consistency. Figure 3 (b) shows SSIM box plot, we can see that `OT_NW` performs similarly with `PMLS` and `L2` scoring highest values while here the median line of `PCT_OT` box lies outside the three top algorithms scoring the lowest value among them. With CID metric in Figure 4, `OT_NW` performs similarly with `PMLS`, `L2` and `PCT_OT`. In conclusion, the quantitative metrics show that our algorithm with Nadaraya Watson `OT_NW` performs similarly with top methods `PMLS`, `L2` and `PCT_OT` and outperforms the rest of the state of the art algorithms.

Figure 7 provides qualitative results. For clarity, the results are presented in image mosaics, created by switching between the target image and the transformed source image column wise (Figure 7, top row). If the colour transfer is accurate, the resulting mosaic should look like a single image (ignoring the small motion displacement between source and target images), otherwise column differences appear. As can be noted, our approach `OT_NW` with Nadaraya Watson step is visually the best at removing the column differences.

While `PMLS` and `PCT_OT` provide equivalent results to our method in terms of metrics measures, `PMLS` on the one hand introduces visual artifacts if the input images are not registered correctly (Figure 6), while our

	PSNR \uparrow						
	IDT 2007	PMLS 2014	GPS/LCP 2018	FGPS/LCP 2018	L2 2019	PCT_OT 2019	OT_NW 5x5
Gangnam1	25.354	35.725	24.048	23.936	35.358	31.479	33.565
Gangnam2	27.116	36.553	25.952	25.944	35.524	35.502	33.627
Gangnam3	22.372	35.007	21.908	21.913	33.284	26.393	28.217
Illum	19.822	20.167	19.785	19.960	19.079	20.306	20.858
Building	20.554	22.634	22.736	22.769	20.499	25.019	24.039
Playground	27.184	27.835	25.501	25.436	27.647	28.482	28.491
Flower1	24.238	26.981	23.765	23.706	26.857	25.186	27.158
Flower2	25.417	25.760	25.259	25.223	25.772	26.373	26.497
Tonal1	30.082	37.215	31.617	31.413	37.332	37.044	37.151
Tonal2	27.992	31.508	25.062	25.087	31.356	32.049	31.579
Tonal3	29.575	36.246	28.136	28.065	36.644	33.793	35.014
Tonal4	28.605	34.521	28.852	28.848	34.344	33.819	35.320
Tonal5	30.330	35.260	29.580	29.448	34.303	36.437	36.616
Mart	22.747	24.742	23.183	23.196	24.450	24.509	25.189
Sculpture	29.884	32.062	29.037	28.820	32.067	31.237	32.735
Mean	26.085	30.814	25.628	25.584	30.301	29.842	30.404
SE	0.905	1.459	0.841	0.821	1.518	1.306	1.291

(a)

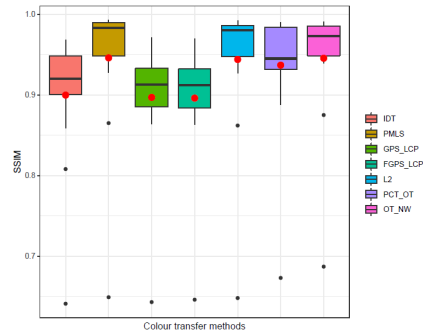


(b)

Figure 2: Metric comparison, using PSNR [14]. (a) Red, blue, and green indicate 1st, 2nd, and 3rd best performance respectively in the table (higher values are better), (b) visualized in box plot (best viewed in colour and zoomed in).

	SSIM \uparrow						
	IDT 2007	PMLS 2014	GPS/LCP 2018	FGPS/LCP 2018	L2 2019	PCT_OT 2019	OT_NW 5x5
Gangnam1	0.900	0.992	0.892	0.891	0.990	0.964	0.973
Gangnam2	0.920	0.993	0.909	0.909	0.986	0.980	0.976
Gangnam3	0.859	0.991	0.873	0.864	0.980	0.930	0.959
Illum	0.641	0.649	0.643	0.646	0.648	0.673	0.687
Building	0.808	0.865	0.864	0.863	0.862	0.888	0.875
Playground	0.920	0.940	0.878	0.876	0.939	0.939	0.943
Flower1	0.909	0.967	0.913	0.912	0.966	0.926	0.959
Flower2	0.901	0.928	0.894	0.894	0.927	0.933	0.939
Tonal1	0.953	0.988	0.971	0.970	0.987	0.988	0.991
Tonal2	0.968	0.987	0.926	0.926	0.986	0.988	0.986
Tonal3	0.962	0.992	0.947	0.946	0.992	0.987	0.990
Tonal4	0.944	0.983	0.932	0.932	0.983	0.981	0.985
Tonal5	0.965	0.986	0.953	0.954	0.985	0.990	0.991
Mart	0.904	0.957	0.925	0.925	0.956	0.941	0.954
Sculpture	0.942	0.971	0.934	0.932	0.972	0.945	0.974
Mean	0.900	0.946	0.897	0.896	0.944	0.937	0.946
SE	0.022	0.023	0.020	0.020	0.023	0.020	0.020

(a)



(b)

Figure 3: Metric comparison, using SSIM [15]. (a) Red, blue, and green indicate 1st, 2nd, and 3rd best performance respectively in the table (higher values are better), (b) visualized in box plot (best viewed in colour and zoomed in).

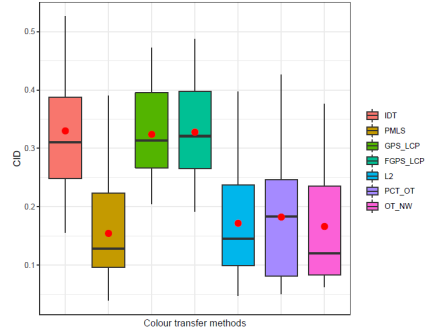
method is robust to registration errors. Note that although the accuracy of the PSNR, SSIM, CID and FSIMc metrics relies on the fact that the input images are registered correctly; if this is not the case, these metrics may not accurately capture all artifacts (Figures 7 and 6). In addition, due to the Nadaraya Watson smoothing step in our algorithm, our approach allows us to create a smoother colour transfer result, and can also alleviate JPEG compression artifacts and noise (cf. Figure 6 for comparison). On the other hand, PCT_OT can create shadow artifacts when there are large changes between target and source images (Figure 6, in example ‘building’), while our method OT_NW can correctly transfer colours between images that contain significant spatial differences and alleviates the shadow artifacts, as can be seen in Figure 6 with examples ‘illum’, ‘mart’ and ‘building’.

5 Conclusion

Several contributions to colour transfer with OT have been made in this paper, showing quantitative and qualitative improvements over state of the art methods. In particular, first, correspondences information as well as colour content of pixels are both encoded in the high dimensional feature vectors, and second, we introduced smoothing as part of the iterative algorithms for solving optimal transport namely Iterative Distribution Transport (IDT) and its variant the Sliced Wasserstein Distance (SWD). The algorithm allows denoising, artifact removal as well as smooth colour transfer between images that may contain large motion changes.

	CID ↓						
	IDT 2007	PMLS 2014	GPS/LCP 2018	FGPS/LCP 2018	L2 2019	PCT_OT 2019	OT_NW 5x5
Gangnam1	0.252	0.040	0.226	0.222	0.048	0.085	0.088
Gangnam2	0.268	0.039	0.291	0.292	0.089	0.068	0.109
Gangnam3	0.496	0.108	0.472	0.487	0.193	0.261	0.267
Illum	0.386	0.390	0.395	0.396	0.397	0.377	0.376
Building	0.374	0.228	0.313	0.321	0.249	0.183	0.275
Playground	0.440	0.238	0.443	0.471	0.254	0.209	0.221
Flower1	0.389	0.163	0.396	0.400	0.174	0.285	0.194
Flower2	0.337	0.245	0.322	0.323	0.266	0.218	0.201
Tonal1	0.310	0.101	0.285	0.308	0.111	0.097	0.063
Tonal2	0.288	0.128	0.351	0.347	0.145	0.099	0.118
Tonal3	0.244	0.079	0.294	0.294	0.081	0.077	0.079
Tonal4	0.240	0.108	0.248	0.238	0.107	0.065	0.065
Tonal5	0.156	0.091	0.205	0.192	0.092	0.051	0.067
Mart	0.526	0.219	0.405	0.402	0.225	0.426	0.249
Sculpture	0.242	0.137	0.213	0.224	0.143	0.232	0.120
Mean	0.330	0.154	0.324	0.328	0.172	0.182	0.166
SE	0.027	0.024	0.022	0.023	0.024	0.031	0.025

(a)

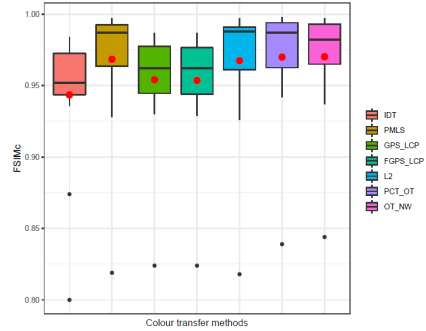


(b)

Figure 4: Metric comparison, using CID [16]. (a) Red, blue, and green indicate 1st, 2nd, and 3rd best performance respectively in the table (lower values are better), (b) visualized in box plot (best viewed in colour and zoomed in).

	FSIMc ↑						
	IDT 2007	PMLS 2014	GPS/LCP 2018	FGPS/LCP 2018	L2 2019	PCT_OT 2019	OT_NW 5x5
Gangnam1	0.936	0.986	0.944	0.943	0.985	0.972	0.979
Gangnam2	0.952	0.992	0.962	0.962	0.988	0.990	0.986
Gangnam3	0.946	0.992	0.962	0.961	0.990	0.987	0.982
Illum	0.800	0.819	0.824	0.824	0.818	0.839	0.844
Building	0.874	0.928	0.930	0.929	0.926	0.942	0.937
Playground	0.950	0.958	0.933	0.932	0.955	0.956	0.960
Flower1	0.954	0.975	0.968	0.967	0.976	0.971	0.977
Flower2	0.941	0.950	0.945	0.945	0.949	0.954	0.956
Tonal1	0.964	0.997	0.986	0.986	0.997	0.998	0.997
Tonal2	0.984	0.993	0.973	0.973	0.992	0.993	0.992
Tonal3	0.979	0.997	0.984	0.983	0.997	0.997	0.995
Tonal4	0.966	0.989	0.972	0.973	0.990	0.995	0.994
Tonal5	0.980	0.994	0.987	0.987	0.993	0.998	0.997
Mart	0.946	0.969	0.960	0.959	0.967	0.969	0.970
Sculpture	0.980	0.987	0.982	0.980	0.988	0.988	0.987
Mean	0.943	0.968	0.954	0.954	0.967	0.970	0.970
SE	0.012	0.012	0.010	0.010	0.012	0.010	0.010

(a)



(b)

Figure 5: Metric comparison, using FSIMc [17]. (a) Red, blue, and green indicate 1st, 2nd, and 3rd best performance respectively in the table (higher values are better), (b) visualized in box plot (best viewed in colour and zoomed in).

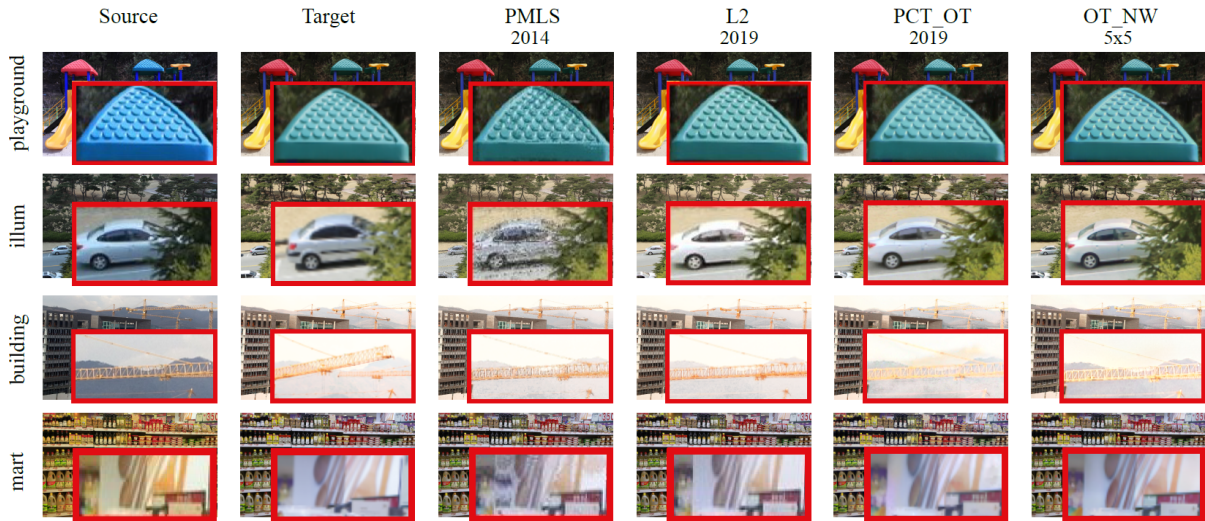


Figure 6: A close up look at some of the results generated using the PMLS, L2, PCT_OT and our algorithm OT_NW (best viewed in colour and zoomed in).

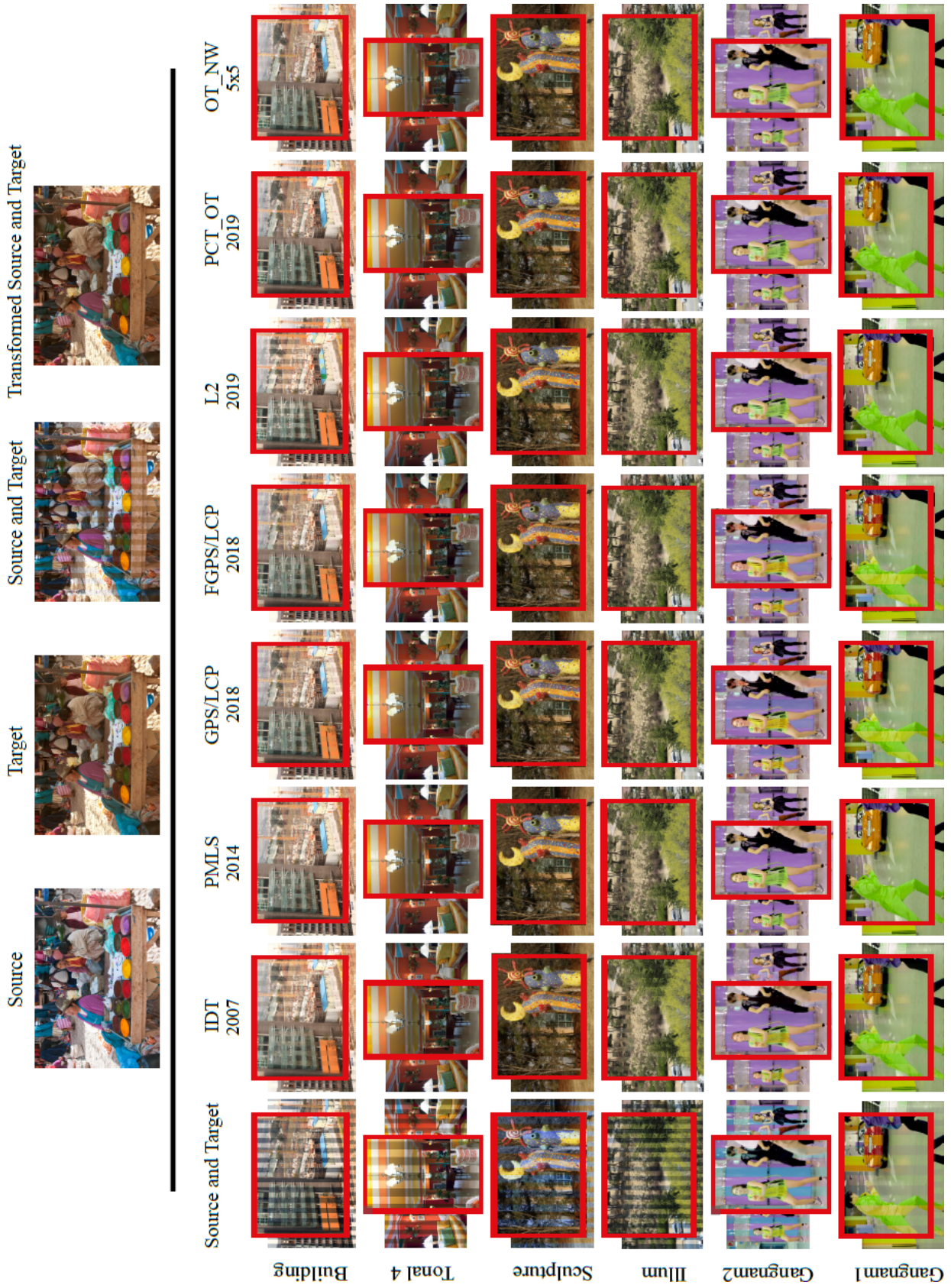


Figure 7: A close up look at some of the results generated using the PMLS, L2, PCT_OT and our algorithm OT_NW (best viewed in colour and zoomed in).

Acknowledgments

This work is partly funded by a scholarship from Umm Al-Qura University, Saudi Arabia, and in part by a research grant from Science Foundation Ireland (SFI) under the Grant Number 15/RP/2776, and the ADAPT Centre for Digital Content Technology (www.adaptcentre.ie) that is funded under the SFI Research Centres Programme (Grant 13/RC/2106) and is co-funded under the European Regional Development Fund.

References

- [1] M. Brown and D. G. Lowe. Automatic panoramic image stitching using invariant features. *International Journal of Computer Vision*, 74(1):59–73, Aug 2007.
- [2] Y. Hwang, J. Lee, I. S. Kweon, and S. J. Kim. Color transfer using probabilistic moving least squares. In *IEEE Conf. on Computer Vision and Pattern Recognition (CVPR)*, pages 3342–3349, June 2014.
- [3] H. Alghamdi, M. Grogan, and R. Dahyot. Patch-based colour transfer with optimal transport. In *2019 27th European Signal Processing Conference (EUSIPCO)*, pages 1–5, Sep. 2019. https://github.com/leshep/PCT_OT.
- [4] C. Liu, J. Yuen, and A. Torralba. Sift flow: Dense correspondence across scenes and its applications. *IEEE Transactions on Pattern Analysis and Machine Intelligence*, 33(5):978–994, May 2011. <https://people.csail.mit.edu/celiu/SIFTflow/>.
- [5] C. Villani. *Optimal transport: old and new*, volume 338. Springer Science & Business Media, 2008.
- [6] Y. Rubner, C. Tomasi, and L. J. Guibas. The earth mover’s distance as a metric for image retrieval. *International Journal of Computer Vision*, 40(2):99–121, Nov 2000.
- [7] F. Santambrogio. Optimal transport for applied mathematicians. *Birkäuser, NY*, pages 99–102, 2015.
- [8] C. Villani. *Topics in optimal transportation*. Number 58. American Mathematical Soc., 2003.
- [9] F. Pitié, A. C. Kokaram, and R. Dahyot. Automated colour grading using colour distribution transfer. *Computer Vision and Image Understanding*, 107(1):123–137, 2007. <https://github.com/frcs/colour-transfer>.
- [10] J. Rabin, G. Peyré, J. Delon, and M. Bernot. Wasserstein barycenter and its application to texture mixing. In *Scale Space and Variational Methods in Computer Vision*, pages 435–446. Springer Berlin Heidelberg, 2012.
- [11] N. Bonneel, J. Rabin, G. Peyré, and H. Pfister. Sliced and radon wasserstein barycenters of measures. *Journal of Mathematical Imaging and Vision*, 51(1):22–45, Jan 2015.
- [12] F. Bellavia and C. Colombo. Dissecting and reassembling color correction algorithms for image stitching. *27(2):735–748*, Feb 2018.
- [13] M. Grogan and R. Dahyot. L2 divergence for robust colour transfer. *Computer Vision and Image Understanding*, 181:39–49, 2019. <https://github.com/groganma/gmm-colour-transfer>.
- [14] D. Salomon. *Data compression: the complete reference*. Springer Science & Business Media, 2004.
- [15] Z. Wang, A. C. Bovik, H. R. Sheikh, and E. P. Simoncelli. Image quality assessment: from error visibility to structural similarity. *13(4):600–612*, April 2004.
- [16] J. Preiss, F. Fernandes, and P. Urban. Color-image quality assessment: From prediction to optimization. *23(3):1366–1378*, March 2014.
- [17] L. Zhang, L. Zhang, X. Mou, and D. Zhang. Fsim: A feature similarity index for image quality assessment. *20(8):2378–2386*, Aug 2011.
- [18] I. Lissner, J. Preiss, P. Urban, M. S. Lichtenauer, and P. Zolliker. Image-difference prediction: From grayscale to color. *22(2):435–446*, Feb 2013.
- [19] M. Oliveira, A. D. Sappa, and V. Santos. A probabilistic approach for color correction in image mosaicking applications. *24(2):508–523*, Feb 2015.
- [20] J. Park, Y. Tai, S. N. Sinha, and I. S. Kweon. Efficient and robust color consistency for community photo collections. In *IEEE Conf. on Computer Vision and Pattern Recognition (CVPR)*, pages 430–438, June 2016.
- [21] M. Xia, J. Y. Renping, X. M. Zhang, and J. Xiao. Color consistency correction based on remapping optimization for image stitching. In *IEEE Int. Conf. on Computer Vision Workshops (ICCVW)*, pages 2977–2984, Oct 2017.